Disassembly of hot classical charged drops

R. J. Lenk and V. R. Pandharipande
Department of Physics, University of Illinois at Urbana-Champaign, Urbana, Illinois 61801
(Received 26 December 1985)

The disassembly of hot classical charged drops containing ~230 and 130 particles is studied with the molecular dynamics method. The strength of the Coulomb repulsion is chosen so that these drops have a binding energy formula similar to that of nuclei. The phase diagram of neutral matter, obtained by switching off the Coulomb force, is also similar to that of nuclear matter. In addition to the total-vaporization, fragmentation, and evaporation modes of the disassembly of neutral drops, the charged drops also break by multiple and binary fission. The liquid-gas phase transition plays an important role in the multiple fission of expanding charged liquid drops. There also appears to be a window in the initial conditions in which binary fission followed by a density oscillation is the dominant mode of breakup. The multiple and binary fission breakups are due to the Coulomb forces, and they yield more massive clusters with relatively few small clusters with ~10 particles. The higher energy fragmentation and total vaporization modes are not significantly influenced by the Coulomb forces. They are primarily due to the liquid-gas transition, and their yields decrease almost monotonically with the number of particles in the cluster.

I. INTRODUCTION

Recent measurements of nuclear fragmentation in high energy proton-nucleus[1] and heavy-ion collisions[2,3] have stimulated theoretical interest in the problem of the disassembly of small hot liquid drops.[4–9] The disassembly of hot nuclei is rather difficult to study microscopically due to their quantum nature, particularly the Fermi statistics and the exchange character of nuclear forces.[9] Nevertheless, many thermodynamic arguments, independent of either the quantum nature or the details of nuclear forces, are used to discuss this phenomenon with the hope that the macroscopic equation of state and the liquid-gas phase transition play an important role.[5,8] Due to the highly dynamic nature of the phenomenon and the small (~200) number of particles involved, it is not obvious that we can use the equation of state of extended matter in thermodynamic equilibrium to discuss the disassembly. In order to gain a better understanding of the relevance of the equation of state and the liquid-gas transition, for the disassembly of small hot liquid drops, Vicentini, Jacucci and Pandharipande[10] (Ref. 10 will henceforth be denoted by I) studied the time evolution of hot drops of Argon containing ~200 atoms by classical molecular dynamics. If we ignore the solid phase, which does not seem to play an important role in the disassembly, the phase diagram of atomic argon (Fig. 1) is similar to that of nuclear matter.[10] However, we note that in this study the classical liquid argon drops are not intended to be mock nuclei, but instead to provide simple systems whose time evolution can be calculated exactly by solving Newton's equations of motion.

The initial state used in I is a sphere containing the prescribed number of atoms, artificially cut out of extended uniform matter at a specific density and temperature. The main conclusions of I may be summarized as follows: The initial expansion of the central matter in the drop is almost adiabatic. If the energy per atom (denoted by e) is small, the expansion is small, and the matter cools by evaporation and recontracts. Density oscillations are highly damped. The magnitude of the expansion increases with e, and large density inhomogeneities develop when the expanding matter enters the region of adiabatic instability. This region is enclosed by the "adiabatic spinodal" (AS) curve in the phase diagram (Fig. 1). If the average central (AC) density ρ_{AC} of the matter in the interior of the drop (called central matter in I) stays greater than $\sim\frac{1}{4}$ of the liquid density, the liquid matter stays connected. At the maximum of the expansion it resembles a liquid blob with a very crooked shape. This blob re-

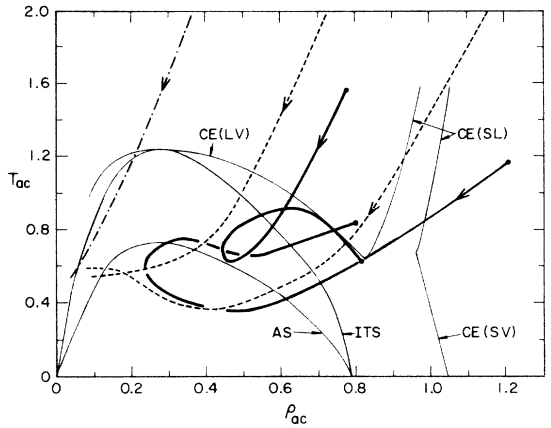

FIG. 1. The phase diagram of neutral matter, and the schematic trajectories of violent evaporation (solid lines), fragmentation (dashed lines), and total vaporization (dash-dot line) of neutral drops having ~230 particles. The coexistence curves are labeled CE and (SL) for solid liquid, (LV) for liquid vapor, and (SV) for solid vapor. The curves ITS and AS show the isothermal and adiabatic spinodals. Density and temperature are in argon natural units.

laxes back to spherical shape; the released surface energy causes significant evaporation. Events of this type were called "violent evaporation" in I. Trajectories of evolution in the ρ_{AC}, T_{AC} plane (T_{AC} denotes the temperature of central matter) for typical neutral events are shown in Fig. 1.

If e is so large that the expansion drives the average density to values <0.2 liquid density, the blob breaks and fragmentation occurs. Generally, a drop with ~ 230 atoms broke into several clusters containing 10 to 60 particles. If e is very large the expanding matter goes above the AS as illustrated in Fig. 1, and totally vaporizes.

In the present work we study the effect of a long range Coulomb repulsion on the disassembly of the hot drop. A q^2/r_{ij} term of appropriate strength is added to the interatomic potential. The strength of the repulsion is adjusted so that liquid argon drops having ~ 300 atoms are unstable against fission. The disassembly of hot charged liquid drops has fission modes in addition to those of evaporation, fragmentation, and vaporization.

The Hamiltonian of the charged drops and the details of the calculation are given in Secs. II and III, and the results are presented in Sec. IV.

II. THE HAMILTONIAN

The time evolution is calculated with the molecular dynamics method[10] using the Hamiltonian:

$$H=\sum_{i=1,A} p_i^2/2m+\sum_{i<j\le A}[v(r_{ij})+q^2/r_{ij}]\,, \tag{2.1}$$

where A is the total number of particles in the drop, and v_{ij} is a truncated Lennard-Jones (LJ) 6,12 potential:

$$v(r_{ij})=4(r^{-12}-r^{-6})-4(3^{-12}-3^{-6}) \text{ for } r<3\,,$$
$$=0 \text{ for } r>3\,. \tag{2.2}$$

The natural units for energy and length of the argon interatomic potential are 119.8 K and 3.405 Å. Neutral matter is defined as is nuclear matter by switching off the Coulomb potential. The equation of state of neutral matter is given in I, and the phase diagram is shown in Fig. 1.

The natural unit of length is approximately the mean interparticle distance at equilibrium. The equilibrium density in natural units is ~ 1; it is 1.04 for argon solid at

TABLE I. Cluster yields of D events. Tables I–IV show results of calculations of the disassembly of charged droplets. Each line is an event, and the events are in order of increasing energy. The events are labeled in the fashion described in Sec. III. Cluster populations are given for the system after 6000 time steps, and are divided into light ($A<7$) and heavy ($A\ge 7$) categories. Light cluster populations are given by N_1-N_6, where N_i is the number of clusters of size i. Heavy cluster populations are given in an explicit list of the cluster sizes present. An asterisk on a heavy cluster, such as 202* in event $D(-0.96, 0.78)$, indicates that the cluster has a growing deformation and hence is likely to fission. E_1 is the average monomer kinetic energy after 6000 steps.

Event (e,T_i)	E_1	Light	Heavy
$D(-1.26, 0.68)$	2.39	17,0,0,0,0,0	211
$D(-1.25, 0.67)$	1.91	20,1,0,0,0,0	204
$D(-1.24, 0.67)$	2.46	20,1,1,0,0,0	203
$D(-1.22, 0.67)$	2.60	19,0,0,0,0,0	208
$D(-1.18, 0.67)$	2.19	12,0,0,0,0,0	67,147
$D(-0.99, 0.78)$	2.11	16,0,0,0,0,0	87,128
$D(-0.97, 0.78)$	2.23	17,3,0,0,0,0	87,119
$D(-0.97, 0.77)$	2.31	15,0,0,0,0,0	92,124
$D(-0.96, 0.78)$	2.31	13,0,1,0,0,0	68,143
$D(-0.96, 0.78)$	2.72	23,2,0,0,0,0	202*
$D(-0.90, 0.78)$	2.39	27,0,0,0,0,0	206*
$D(-0.75, 0.88)$	2.33	27,0,0,0,0,0	23,36,57,86
$D(-0.74, 0.90)$	2.04	22,2,0,0,0,0	17,78,110
$D(-0.69, 0.82)$	2.33	24,1,0,0,0,1	48,67,77
$D(-0.65, 0.88)$	1.98	19,0,0,0,0,0	21,32,39,46,73
$D(-0.63, 0.88)$	2.03	32,3,0,0,0,1	20,166
$D(-0.62, 0.89)$	2.67	29,2,0,0,0,0	84,112
$D(-0.59, 0.88)$	2.04	25,1,0,0,0,0	22,25,35,45,72
$D(-0.58, 0.82)$	1.92	29,2,0,0,0,0	53,70,71
$D(-0.19, 1.10)$	2.44	39,4,0,1,0,0	18,29,35,95
$D(0.42, 1.32)$	2.82	47,2,0,1,1,1	7,11,11,14,14,15,20,29,45
$D(1.16, 1.56)$	3.27	50,6,1,0,2,0	8,13,13,15,15,16,16,18,19,22
$D(1.63, 1.77)$	3.26	66,5,5,1,1,0	7,9,10,14,20,33,36
$D(2.45, 2.22)$	4.52	64,9,6,3,2,2	11,12,14,16,18,19
$D(4.74, 2.88)$	6.65	96,13,4,3,3,2	7,7,7,9,9,10,11
$D(6.23, 3.53)$	8.78	85,17,10,7,1,1	7,8,8,12

$T=0$, and 0.82 for argon liquid at $T=0.7$. With this criterion the natural length unit for nuclear matter should be 1.8 fm. It is more difficult to define an analogous natural unit of energy in nuclear matter. The binding energy is ~ 6 per particle in natural units; it is ~ 8 for solid, and ~ 5 for liquid argon. With this criterion the natural energy unit for nuclear matter will be ~ 2.5 MeV. However, the critical temperature of argon is 1.3 in natural units, while that of nuclear matter is ~ 17 MeV.

We have used the value $q^2=0.055$ (in argon natural units) in our work. This value is obtained by comparing the expansion of the binding energy of solid charged argon granules, in powers of $A^{-1/3}$, with that of nuclei. The binding energy per atom of a cold neutral hexagonal close-packed (hcp) argon crystal, with the truncated LJ potential is -8.3. The energy of a surface parallel to hcp planes is 2.37 per unit area, and the unit radius $r_0=0.61$. From these we obtain the binding energy formula:

$$E/A \sim -8.3+11A^{-1/3}+0.054A^{2/3} , \tag{2.3}$$

that is not too different from the nuclear binding energy formula:

$$E/A \sim -15+18A^{-1/3}+0.12A^{2/3}\ (\text{MeV}) . \tag{2.4}$$

Both equations (2.3) and (2.4) are rather crude. In (2.3) we have used the energy of a surface parallel to the hexagonal Bravais planes instead of that of a truly spherical surface, while in (2.4) we have approximated the dependence of nuclear binding energies on neutron and proton number by taking the proton fraction to be 0.4.

The surface tension of liquid argon at the melting temperature $T=0.7$ is estimated[11] to be 1.28. In fact this is the tension of the planar interface between vapor and liquid phases in equilibrium. Thus using it for a quasistable (or evaporating) surface dividing the liquid phase and vacuum is an approximation. We note that the surfaces involved in the study of dissociation of hot drops are at best quasistable. Empirically the surface tension of liquids at temperature T is given by

$$\sigma(T)=\sigma_0[\rho_L(T)-\rho_G(T)]^4 , \tag{2.5}$$

where $\rho_L(T)$ and $\rho_G(T)$ are the densities of the liquid and gas phases on the coexistence curve at temperature T. At small T the $\rho_G(T)$ is negligible, and the tension of the surface in equilibrium may not be too different from that of the quasistable surface in vacuum. At larger values of T, however, the tension of an evaporating surface can be significantly different from that of a surface in equilibrium.

The stability of charged liquid drops is given by the classical Bohr-Wheeler criterion:

$$\frac{2E(\text{surface})}{E(\text{Coulomb})} > 1 . \tag{2.6}$$

At low temperatures where $\rho_G(T)$ is small, we can use the equilibrium surface tension to estimate the surface energy. At $T=0.7$ we obtain:

$$\frac{2E(\text{surface})}{E(\text{Coulomb})} \sim \frac{290}{A} , \tag{2.7}$$

TABLE II. Cluster yields of B events. See the caption for Table I.

Event (e,T_i)	E_1	Light	Heavy
$B(-1.96, 0.47)$	3.25	2,0,0,0,0,0	229
$B(-1.37, 0.68)$	2.67	14,0,0,0,0,0	218
$B(-0.99, 0.91)$	2.47	18,3,1,0,0,0	204
$B(-0.95, 0.90)$	2.29	24,0,1,0,0,0	193
$B(-0.89, 0.90)$	2.35	34,3,0,0,0,0	191
$B(-0.84, 0.88)$	2.38	27,2,0,0,0,0	200
$B(-0.84, 0.90)$	2.65	27,3,1,0,0,0	195
$B(-0.44, 1.14)$	2.64	43,5,1,0,0,1	168
$B(-0.36, 1.13)$	2.40	44,6,0,0,0,0	170
$B(-0.32, 1.12)$	2.68	46,2,0,0,0,0	34,143
$B(-0.28, 1.15)$	2.39	46,2,0,1,0,0	61,111
$B(-0.20, 1.12)$	3.09	37,7,0,0,0,0	13,165
$B(-0.14, 1.26)$	2.36	46,5,2,0,1,0	157
$B(-0.03, 1.27)$	2.55	49,4,1,0,1,0	15,40,104
$B(-0.01, 1.26)$	2.44	43,7,3,0,0,0	8,35,59,60
$B(0.04, 1.23)$	1.94	42,2,1,1,2,0	8,10,11,54,76
$B(0.04, 1.26)$	3.01	58,4,2,0,0,0	12,141
$B(0.04, 1.26)$	2.17	54,7,1,1,0,0	66,76
$B(0.04, 1.27)$	2.53	53,2,3,1,1,0	8,143
$B(0.27, 1.38)$	2.98	55,0,1,0,0,0	8,10,11,30,34,38,41
$B(1.48, 1.90)$	3.42	69,11,4,0,1,3	7,7,8,8,12,17,18,24
$B(2.48, 2.48)$	3.91	82,11,5,2,2,3	7,8,9,12,12,15,15
$B(4.74, 3.31)$	6.28	97,24,5,3,3,4	11
$B(6.08, 4.22)$	7.55	133,18,6,5,0,0	12
$B(8.44, 5.40)$	9.89	135,17,9,2,1,0	7
$B(25.00, 13.60)$	26.75	196,10,1,0,0,0	

TABLE III. Cluster yields of d events. See the caption for Table I.

Event (e,T_i)	E_1	Light	Heavy
$d(-1.17, 0.78)$	1.65	16,1,0,0,0,0	113
$d(-1.16, 0.88)$	1.76	16,2,0,0,0,0	111
$d(-1.08, 0.87)$	1.94	18,0,0,0,0,0	12,100
$d(-1.08, 0.88)$	2.30	21,2,0,0,0,0	108
$d(-0.94, 1.00)$	2.52	18,0,0,0,0,0	113
$d(-0.89, 0.88)$	2.05	22,0,1,0,0,0	28,80
$d(-0.79, 0.88)$	2.20	22,1,0,1,1,0	102
$d(-0.70, 1.01)$	1.90	27,0,0,0,0,0	106*
$d(-0.69, 1.11)$	1.75	24,2,1,0,0,0	30,69
$d(-0.68, 1.00)$	1.78	27,0,0,0,0,0	40,64
$d(-0.68, 1.00)$	2.02	20,0,1,0,0,0	54,55
$d(-0.57, 1.11)$	2.23	19,0,0,1,1,0	14,17,71
$d(-0.46, 1.02)$	1.88	24,3,0,0,0,0	12,19,32,39
$d(-0.36, 1.11)$	2.27	29,0,1,1,0,0	35,58
$d(-0.33, 1.11)$	2.39	26,0,0,0,0,0	10,21,25,50
$d(-0.25, 1.22)$	1.80	26,3,0,0,0,1	8,9,27,49
$d(-0.06, 1.22)$	2.09	28,2,0,0,0,1	14,15,17,20,32
$d(-0.01, 1.07)$	1.98	30,3,0,0,0,1	12,16,17,22,23
$d(0.37, 1.26)$	2.25	40,2,0,0,1,1	7,26,45
$d(1.67, 1.79)$	3.42	34,7,1,1,2,1	7,7,8,10,11,18
$d(2.25, 2.18)$	4.28	41,8,2,3,2,1	9,9,17
$d(4.99, 3.51)$	7.11	66,9,4,3,0,0	7,7,9

TABLE IV. Cluster yields of b events. See the caption for Table I.

Event (e,T_i)	E_1	Light	Heavy
$b(-1.74, 0.72)$	1.50	6,0,0,0,0,0	124
$b(-1.34, 0.92)$	2.18	14,0,0,0,0,0	117
$b(-1.28, 0.89)$	1.70	10,2,0,0,0,0	34,84
$b(-1.15, 0.91)$	2.14	13,2,0,0,0,0	115
$b(-1.08, 0.87)$	1.65	14,1,1,0,0,0	106
$b(-1.06, 0.87)$	2.22	19,0,0,0,0,0	113
$b(-0.80, 1.12)$	2.22	27,1,0,0,0,0	100
$b(-0.67, 1.16)$	1.90	26,3,1,0,0,0	96
$b(-0.63, 1.14)$	2.36	30,2,0,0,0,0	99
$b(-0.62, 1.12)$	2.05	26,2,1,0,0,0	92
$b(0.12, 1.36)$	2.18	42,0,2,0,0,1	77
$b(1.46, 1.85)$	3.50	49,4,1,4,1,1	7,15,17
$b(1.72, 2.42)$	3.73	53,6,4,1,0,0	9,10,25
$b(5.97, 4.22)$	7.71	81,8,6,1,1,1	

TABLE V. Cluster yields of neutral and charged events with similar ρ_i and T_i. Letters N and C in the event label denote neutral and charged events. See the caption of Table I for other details.

Event (e,T_i)	Light	Heavy
$D(-1.6, 1.29)N$	33,5,0,1,0,0	183
$D(0.42, 1.32)C$	47,2,0,1,1,1	7,11,11,14,14,15,20,29,45
$B(-0.72, 1.95)N$	74,4,2,1,1,0	134
$B(1.48, 1.90)C$	69,11,4,0,1,3	7,7,8,8,12,17,18,24
$D(0.42, 2.23)N$	67,7,3,0,2,0	7,7,11,11,12,16,16,24
$D(2.45, 2.22)C$	64,9,6,3,2,2	11,12,14,16,18,19
$B(0.63, 2.54)N$	85,15,6,1,0,1	7,9,10,14,19,31
$B(2.48, 2.48)C$	82,11,5,2,2,3	7,8,9,12,12,15,15
$B(6.89, 5.58)N$	140,22,6,2,3,0	
$B(8.44, 5.40)C$	135,17,9,2,1,0	7

which is quite close to that for nuclei ($Z=0.4A$)

$$\frac{2E(\text{surface})}{E(\text{Coulomb})} \sim \frac{300}{A} . \tag{2.8}$$

The charged drops will certainly become more unstable at higher temperatures because the $\sigma(T)$ of even the quasi-stable surface is expected to decrease as T increases.

III. CALCULATIONS

The present calculations are quite similar to those reported in I. The Coulomb force is switched off, and a cube containing 432 (250) particles is equilibrated under periodic boundary conditions at the desired density and temperature. At time $t=0$ the Coulomb force is turned on, and all particles outside of a sphere, whose diameter equals the side of the cube, are removed along with the periodic boundary conditions. This sphere contains ~ 230 (130) particles, and forms our initial state. The time evolution of the particles is followed by molecular dynamics with a time step of 10^{-14} sec. The cluster composition at any chosen time t is determined from the positions of the particles at time t. Briefly, a cluster is defined so that it is possible to go from any particle i to another particle i' belonging to the same cluster by successive interparticle jumps of distance $<d$. The final composition is not too sensitive to d when d is in the range 2–3. The range of the strong interaction (2.2), which is responsible for the binding of the clusters, is 3, so that d cannot be greater than 3. We use $d=3$ in the present work.

The "central matter" is defined as that consisting of half of the particles belonging to the largest cluster that are closest to the center of mass of that cluster. Before fragmentation or fission most of the particles belong to a single large cluster. The density ρ_{AC} and temperature T_{AC} of the central matter is measured as in I. After fragmentation, or the formation of fission neck, the present definitions of ρ_{AC} and T_{AC} become less meaningful. For example, all the particles in a system with a well-developed fission neck belong to a single large cluster. The center of mass of this cluster is close to the neck, and so the present definition of the "central matter" is not meaningful. The time evolution of the central matter is shown on ρ, T planes by trajectories of $\rho_{AC}(t)$, $T_{AC}(t)$.

Events with initial densities of 0.82 and 1.2, with ~ 230 (130) atoms, are respectively, labeled by letters B and D (b and d), the values of e, the total energy per atom, and T_i, the initial temperature. Thus $D(-0.63, 0.88)$ denotes an event in which a charged hot liquid drop containing ~ 230 atoms having $\rho_i=1.2$, $e=-0.63$, and $T_i=0.88$ dissociated. The energy e is conserved, and it is important in the analysis of the events. In I only e and ρ_i are included in the event label, and values of T_i are listed in the tables. We find that T_i is useful to compare neutral and charged events. Also, while comparing neutral and charged events, we add the letters N and C to the event labels to differentiate them.

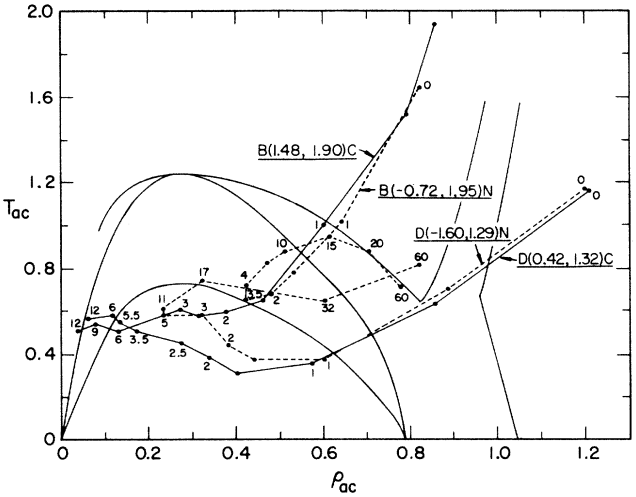

FIG. 3. Evolution trajectories of neutral (dashed lines) and charged (solid lines) events having similar T_i. In the temperature region covered by this figure, the charged drops fragment, but the neutral drops do not.

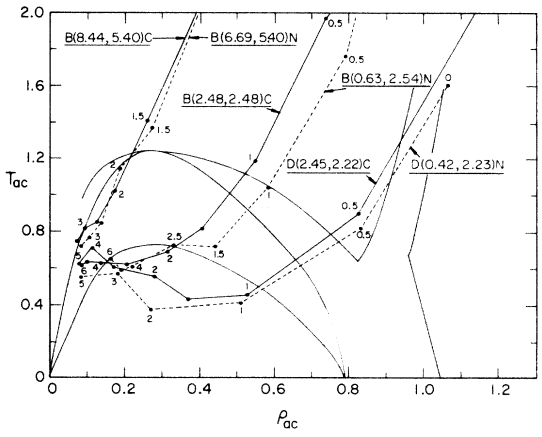

FIG. 2. Evolution trajectories of neutral (dashed lines) and charged (solid lines) events having $T_i>2$. The top two trajectories show total vaporization, while the others give fragmentation. The dots on the trajectories give time in units of 100 steps. Thus a dot labeled 2 gives ρ_{AC} and T_{AC} at $t=200$ steps.

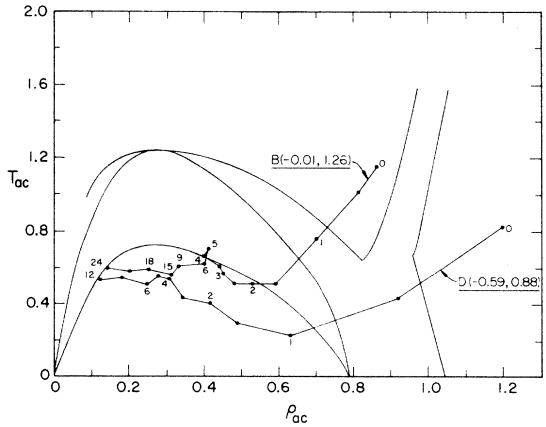

FIG. 4. Trajectories of multiple fission events of charged drops. Note that the expansion almost stops at $t\sim 400$ steps when the central density is $\sim \frac{1}{2}$ the liquid density.

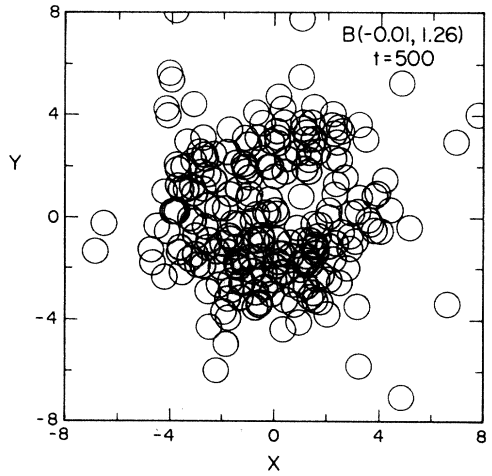

FIG. 5. The x,y coordinates of the particles, in natural units, at time $t=500$ steps in the multiple fission event $B(-0.01, 1.26)$. The circles representing the particles have diameter of ~ 1, which is the radius of the repulsive core in the two-body interaction in natural units. The drop has a horseshoe type of shape.

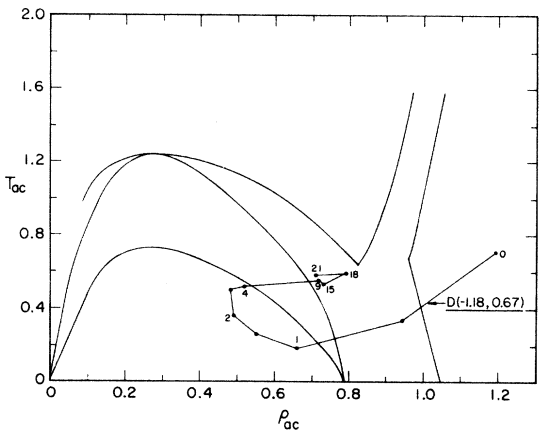

FIG. 7. Evolution trajectory of the fast fission event $D(-1.18, 0.67)$. The present definitions of the ρ_{AC} and T_{AC} have doubtful validity after $t=2100$ steps. The distribution of particles at $t=1500$ steps is shown in Fig. 8.

IV. RESULTS

The cluster compositions at $t=6000$ steps are given in Tables I–IV. Events such as $D(-0.99, 0.78)$ have clearly undergone binary fission, while those like $D(-0.69, 0.82)$ are examples of ternary fission. The composition of events with $e>-0.5$ appeared to have stabilized by $t=6000$, while that of events having $e<-0.5$ has not necessarily stabilized. For example, in the event $D(-0.90, 0.78)$ the deformation of the drop with 206 particles was growing at $t=6000$. We expect that it will fission at a later time. Events that have the same macroscopic initial states, i.e., their ρ_i, e_i, and T_i are identical, do not necessarily give the same final state, as can be seen by comparing the composition of the two $D(-0.96, 0.78)$ events in Table I. To obtain identical final states the initial states must be microscopically identical, i.e., the initial positions and the velocities of all the particles must be identical.

The cluster compositions of some neutral (from Ref. I) and charged events at relatively high initial temperatures are compared in Table V. The Coulomb energy of the initial states is ~ 2 per particle for B and D events, and it accounts for the difference in energy between charged and neutral events. In total vaporization events, such as $B(6.89, 5.58)N$ (neutral) and $B(8.44, 5.40)C$ (charged), the Coulomb force does not seem to play a major role. The effect of Coulomb force on higher-energy fragmentation events, having $T_i>2$, also appears to be small. The fragmentation of the charged drops seems to produce clusters of a slightly smaller size. The trajectories of neutral and charged events with $T_i>2$ are compared in Fig. 2.

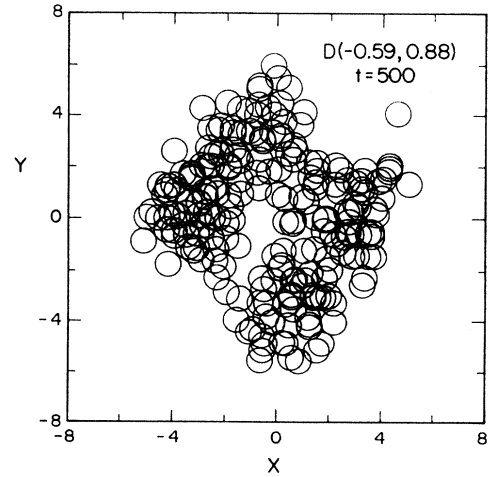

FIG. 6. The x,y coordinates of the particles at time $t=500$ steps in the multiple fission event $D(-0.59, 0.88)$. See the caption of Fig. 5 for more details.

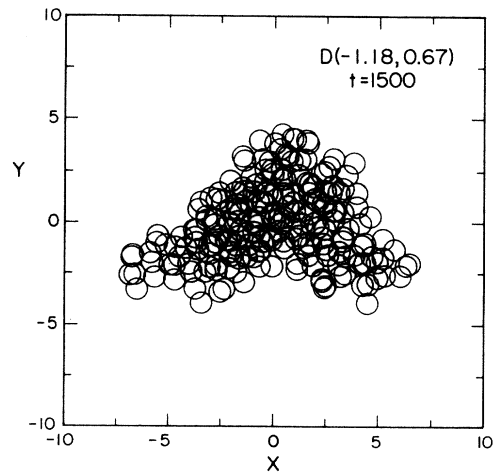

FIG. 8. The x,y coordinates of the particles at time $t=1500$ steps in the fast fission event $D(-1.18, 0.67)$. The evolution trajectory is shown in Fig. 7.

The significant effects of the Coulomb force are seen at lower T_i. The neutral events $B(-0.72, 1.95)N$ and $D(-1.6, 1.29)N$ are classified as violent evaporations in I. The corresponding charged events $B(1.48, 1.90)C$ and $D(0.42, 1.32)C$, however, undergo fragmentation. The trajectories of these events are compared in Fig. 3. The extra Coulomb repulsion pushes the expansion to values of ρ_{AC} less than 0.2, where the system fragments.

At lower energies, in the range of $-0.2 > e > -0.8$ for D events and $e \sim 0$ in B events, the evolution of the charged system is qualitatively different from that of the neutral system. The charged system expands into the region of adiabatic instabilities, but it does not have enough energy to expand to low values of ρ_{AC}. The expansion stops, or becomes very slow, in the region $\rho_{AC} \sim 0.3$ to $0.5\rho_L$, and the system phase separates with a slight rise in temperature. For example in both the events shown in Fig. 4, phase separation seems to occur in the region of $t \sim 400$ steps. The condensed liquid has a crooked shape (Figs. 5 and 6), but it is a single connected body. However, instead of relaxing back to spherical shape as the neutral system did, the crooked liquid drop breaks into a few big clusters due to the Coulomb repulsion. This process can be called multiple fission because it is primarily due to the Coulomb repulsion. It yields fewer and more massive clusters than the typical fragmentation events (Tables I–IV).

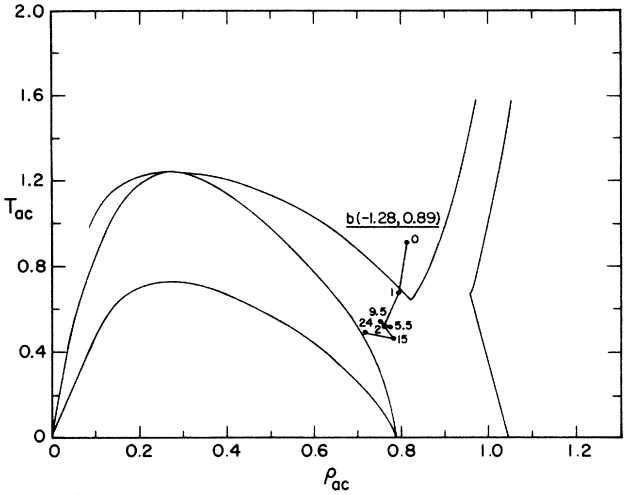

FIG. 9. The evolution trajectory of the fission event $b(-1.28, 0.89)$.

At still lower energies, $e \sim -1.0$ in D events and $e \sim -0.3$ in B events, we find binary fission with very

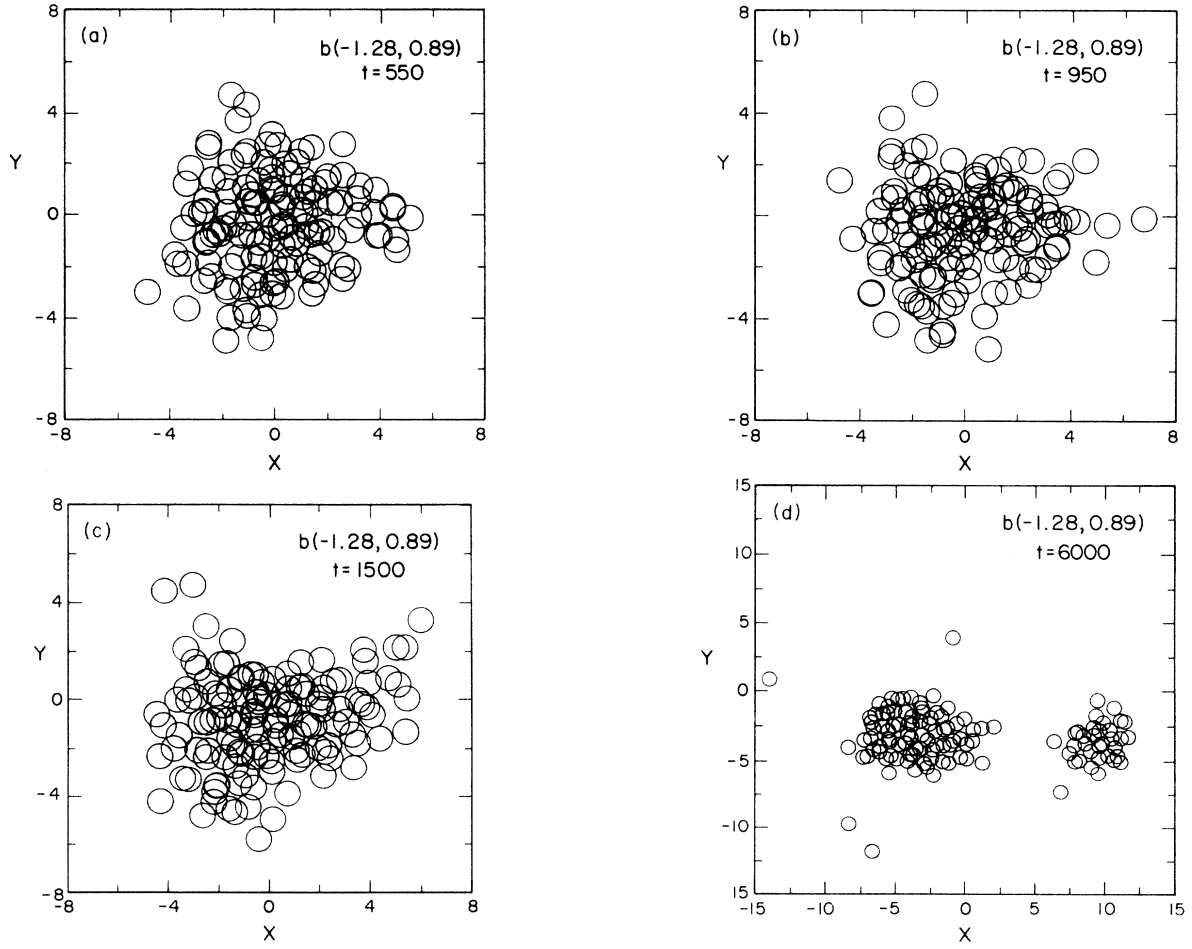

FIG. 10. The x, y coordinates of the particles at $t = 550$, 950, 1500, and 6000 steps in the fission event $b(-1.28, 0.89)$ are shown in parts (a), (b), (c), and (d), respectively.

high probability. This fission occurs in a small energy window via the following mechanism. The system expands and recontracts (Fig. 7). If the energy is above the window the system will undergo multiple fission without recontraction. If e is within the window, the system is likely to recondense with a high degree of deformation (Fig. 8). This deformation slowly increases and the system fissions into two big clusters. If the energy is too small, the expansion is not large, and the system is likely to recontract into an almost spherical shape. These systems do not fission with a large probability in the time scale considered in this work. We note that in 6000 units of time a sound wave travels ~ 20 times across the drop with 230 particles. We refer to fission, such as that of event $D(-1.18, 0.67)$, following a significant density oscillation as "fast fission" because it occurs on these short time scales.

At lower energies we can expect the more conventional "spontaneous" mode of fission in which a thermal fluctuation causes a critical deformation of the shape. We have found only one possible candidate for this process; the event $b(-1.28, 0.89)$. Its evolution trajectory is shown in Fig. 9, and the time evolution of particle positions is shown in Figs. 10(a)–(d). In this event the drop, after a small initial expansion, appears to have stabilized. It stays for ~ 2000 steps (from ~ 200 to 2200) at $\rho_{AC} \sim 0.8$ and $T_{AC} \sim 0.5$, and fissions. It is likely that some of the large residues in other low energy events may undergo spontaneous fission at $t > 6000$. The fraction of spontaneous fission occurrence at sufficiently low energies will be determined by a competition between evaporation cooling and fission.

In conclusion we find that at lower energies the disassembly of hot liquid drops is significantly influenced by the Coulomb repulsion. In addition to the vaporization, fragmentation, and evaporation modes of neutral drops, the disassembly of charged drops has multiple and binary fission modes. Clusters with many (> 20) particles are produced in these fission modes, with relatively few clusters having ~ 10 particles. In particular circumstances, D events with $e = -0.97$ and $T_i = 0.78$, for example, binary fission following a density oscillation occurs with a very large probability. The observed mass yields in the ^{12}C-induced reactions on gold[2] show a dip at $Z \sim 12$. The present studies suggest that this dip could be due to multiple or binary fission of the compound system. Mass yields obtained from the disassembly of charged hot drops are being studied by simulating a large number of events with the same macroscopic initial condition.

The authors wish to thank Professor G. Jacucci for his interest and help in this research supported by the National Science Foundation, Grant PHY84-15064.

[1] J. E. Finn, *et al.*, Phys. Rev. Lett. **49**, 1321 (1982); R. W. Minisch *et al.*, Phys. Lett. **118B**, 458 (1982).
[2] C. B. Chitwood *et al.*, Phys. Lett. **131B**, 289 (1983).
[3] A. I. Warwic *et al.*, Phys. Rev. C **27**, 1083 (1983).
[4] J. Hüfner, Phys. Rep. **125**, 129 (1985).
[5] G. Bertsch and P. J. Siemens, Phys. Lett. **126B**, 9 (1983).
[6] A. D. Panagiotou *et al.*, Phys. Rev. Lett. **52**, 496 (1984).
[7] A. L. Goodman, J. I. Kapusta, and A. Z. Mekjian, Phys. Rev. C **30**, 851 (1984).
[8] J. A. Lopez and P. J. Siemens, Nucl. Phys. **A431**, 728 (1984).
[9] S. Das Gupta, C. Gale, and J. Gallego, Phys. Rev. C **33**, 1634 (1986).
[10] A. Vicentini, G. Jacucci, and V. R. Pandharipande, Phys. Rev. C **31**, 1783 (1985).
[11] F. A. Abraham, Phys. Rep. **53**, 93 (1979).